

# Fluorescence-dip infrared spectroscopy of tropolone and tropolone-OD

Rex K. Frost, Fredrick C. Hagemester, Caleb A. Arrington, and Timothy S. Zwier<sup>a)</sup>  
*Department of Chemistry, Purdue University, West Lafayette, Indiana 47907-1393*

Kenneth D. Jordan<sup>a)</sup>  
*Department of Chemistry, University of Pittsburgh, Pittsburgh, Pennsylvania 15260*

(Received 13 March 1996; accepted 7 May 1996)

Fluorescence-dip infrared spectroscopy (FDIRS) is employed to record the infrared spectra of the isolated, jet-cooled tropolone molecule (TrOH) and its singly deuterated isotopomer TrOD in the O–H and C–H stretch regions. The ability of the method to monitor a single ground-state level enables the acquisition of spectra out of the lower and upper levels of the zero-point tunneling doublet free from interference from one another. The high power of the optical parametric oscillator used for infrared generation produces FDIR spectra with good signal-to-noise despite the weak intensity of the C–H and O–H stretch transitions in tropolone. The expectation that both spectra will exhibit two OH stretch transitions separated by the OH( $v=1$ ) tunneling splitting is only partially verified in the present study. The spectra of TrOH are compared with those from deuterated tropolone (TrOD) to assign transitions due to C–H and O–H, which are in close proximity in TrOH. The appearance of the spectra out of lower ( $a_1$  symmetry) and upper ( $b_2$  symmetry) tunneling levels are surprisingly similar. Two sharp transitions at  $3134.9\text{ cm}^{-1}$  (out of the  $a_1$  tunneling level) and  $3133.9\text{ cm}^{-1}$  (out of the  $b_2$  tunneling level) are separated by the ground-state tunneling splitting ( $0.99\text{ cm}^{-1}$ ), and thereby terminate in the same upper state tunneling level. Their similar intensities relative to the C–H stretch transitions indicate that the  $y$ - and  $z$ -polarized transitions are of comparable intensity, as predicted by *ab initio* calculations. The corresponding transitions to the other member of the upper state tunneling doublet are not clearly assigned by the present study, but the broad absorptions centered about  $12\text{ cm}^{-1}$  below the assigned transitions are suggested as the most likely possibility for the missing transitions. © 1996 American Institute of Physics. [S0021-9606(96)01731-X]

## I. INTRODUCTION

Tropolone (TrOH) is a seven-membered pseudo-aromatic notable for its hydrogen-atom tunneling in a symmetric double minimum potential well.<sup>1–7</sup> The ready wavelength accessibility, reasonable fluorescence quantum yield, and low H-atom tunneling barrier of the  $S_1$  state of tropolone produces  $S_1$  tunneling splittings which are easily observed and probed on a single vibronic level basis. In tropolone and its symmetric derivatives,<sup>8–10</sup> tunneling splittings are increased significantly by excitation of vibrations such as  $\nu_{13}$  and  $\nu_{14}$  which have significant C–O/C=O in-plane wag character, while several other modes effectively suppress the tunneling. Such vibrational mode specificity carries over to slightly asymmetric derivatives such as 5-hydroxytropolone,<sup>11–13</sup> where the localized syn and anti isomers in the ground state become strongly mixed in the  $S_1$  state following excitation of one or more quanta of a C–O/C=O in-plane wag “promoter mode.” This enhancement arises because the symmetric C–O in-plane wag modulates the O–O distance, and the H-atom tunneling rate is sensitively dependent on this distance.

In the search for vibrationally mode-specific effects on H-atom tunneling, the O–H stretch is anticipated to be of considerable importance since it, perhaps more than any other mode, is associated with the tunneling reaction

coordinate.<sup>14,15</sup> In the  $S_1 \leftarrow S_0$  spectroscopy, direct excitation of the OH stretch in  $S_1$  is not easily detected due to the low fluorescence quantum yield of levels so far above the electronic origin and/or poor Franck–Condon factors for the transition. On the other hand, the OH stretch transition is infrared allowed in the ground state. Its excitation in  $S_0$  will probe regions of the potential energy surface where tunneling may be facile and where intramolecular couplings will play a largely unexplored role in the tunneling dynamics. Such a prospect fuels the present study.

The OH stretch region in tropolone has been studied in the matrix<sup>2</sup> and at room temperature in the gas phase.<sup>3</sup> The OH stretch transition(s) have proven remarkably elusive. As shown in Fig. 1, a quartet of transitions is predicted, with spacings determined by the OH( $v=0$ ) and OH( $v=1$ ) tunneling splittings. The polarization of the bands which make up the quartet is given in the figure ( $y$  or  $z$ ). Since the intensity of the bands is related to the component of the dipole moment derivatives along these axes, intensity differences are anticipated which could provide a clue to their assignment.

Tentative assignment of a weak, broad band at  $3121\text{ cm}^{-1}$  in a neon matrix<sup>2</sup> ( $3140\text{ cm}^{-1}$  in the room temperature gas phase spectrum<sup>3</sup>) to the OH stretch transition of TrOH has been made, but the second predicted band separated from the first by the OH( $v=1$ ) tunneling splitting has not been observed. When the tunneling hydrogen in tropolone is deu-

<sup>a)</sup>Authors to whom correspondence should be addressed.

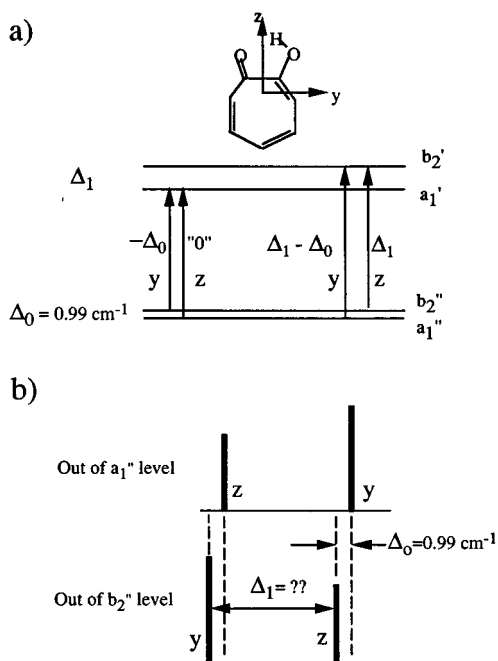


FIG. 1. (a) Schematic energy level diagram for the OH stretch ( $v=0$ ) and ( $v=1$ ) tunneling levels. The relative frequency and polarization ( $y$  or  $z$ ) of the quartet of transitions are labelled, where  $\Delta_v$  is the tunneling splitting in the  $v$ th OH stretch level. (b) Stick diagram of the qualitative positions and intensities of the OH( $v=0-1$ ) tunneling quartet. The intensities are taken from the simple model for the tunneling wave functions outlined in the discussion section.

tered (TrOD) in the matrix studies, a doublet at  $2326$  and  $2345\text{ cm}^{-1}$  is assigned to the OD stretch and serves largely as the basis for the assignment of the  $3121\text{ cm}^{-1}$  band to the OH stretch. Redington and Redington<sup>2</sup> have used the TrOD matrix data to predict a  $50\text{ cm}^{-1}$  OH( $v=1$ ) tunneling splitting in TrOH, but no experimental verification has yet been made. The present study probes the O–H stretch region of the jet-cooled, isolated tropolone molecule. Furthermore, by employing fluorescence-dip infrared spectroscopy,<sup>16</sup> infrared spectra out of the lower and upper tunneling levels can be recorded free from interference from one another.

A second motivation of the present work is to compare the spectral properties of the intramolecular OH $\cdots$ O hydrogen bond in jet-cooled tropolone with those of intermolecular OH $\cdots$ O hydrogen bonds in cold, gas-phase complexes.<sup>17–22</sup> The OH stretch absorption in the infrared provides an important diagnostic of OH $\cdots$ X hydrogen bonds. When the hydrogen bond is intermolecular, the strength of the hydrogen bond is reflected in (i) the magnitude of the frequency shift of the OH stretch absorption, (ii) an increase in the integrated absorption strength of the band (often by a factor of 5 or more), and (iii) an increase in the breadth of the O–H stretch absorption, which can often spread over hundreds of wave numbers in the condensed phase.<sup>24</sup> Recent experiments by our group<sup>19,20</sup> and others<sup>21–23</sup> are providing O–H stretch infrared spectra of size-selected hydrogen-bonded clusters in the gas phase. These spectra are bringing

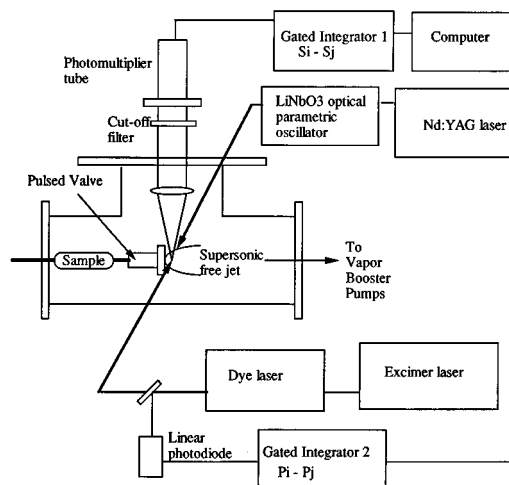


FIG. 2. Experimental apparatus used for fluorescence-dip infrared spectroscopy.

a new perspective to the near-infrared spectra of intermolecularly hydrogen-bonded aggregates.

Molecules which incorporate an intramolecular O–H $\cdots$ X hydrogen bond typically show a large red shift in the O–H stretch frequency (i.e., toward lower frequency), but only a modest increase in the intensity of the transition.<sup>24,25</sup> By studying the O–H stretch transitions in the jet-cooled molecule, the similarities and differences of intermolecular and intramolecular hydrogen bonds can be probed under the idealized conditions of supersonic expansion cooling.

Finally, in the two adjoining papers, O–H stretch infrared spectra are reported for the tropolone-H<sub>2</sub>O complex by our group, while Mitsuzuka *et al.*<sup>26</sup> also explore this complex and extend the data to include tropolone-(H<sub>2</sub>O)<sub>*n*</sub> and tropolone-(CH<sub>3</sub>OH)<sub>*n*</sub> clusters up to  $n=3$ .

## II. EXPERIMENT

The infrared spectra of TrOH and TrOD are recorded using the double resonance method called fluorescence-dip (or fluorescence-detected) infrared spectroscopy (FDIRS), the fluorescence-based analog of resonant ion-dip infrared spectroscopy (RIDIRS). This method has been recently employed by Ebata *et al.*<sup>22</sup> in recording  $S_0$  and  $S_1$  state OH stretch infrared spectra of phenol-(H<sub>2</sub>O)<sub>*n*</sub> clusters with  $n=1$  and 3. In the case of tropolone, fluorescence-based detection is used because the  $S_1$  state is less than halfway to the ionization potential, requiring two-color methods in a RIDIR experiment. FDIRS relies on wavelength selectivity alone for species selection.

The vacuum chamber, excimer-pumped dye laser used for the fluorescence step,<sup>12</sup> and LiNbO<sub>3</sub> optical parametric oscillator (OPO) used as infrared source,<sup>19</sup> have all been described previously. The present discussion focuses on the FDIRS implementation itself, which is shown schematically in Fig. 2. Cold, gas-phase tropolone molecules are formed in a pulsed supersonic expansion either with gentle heating of the tropolone sample or at room temperature. The population

in a single ground-state vibrational level is monitored by choice of the appropriate transition in the fluorescence excitation spectrum. The excimer-pumped dye laser operates at 40 Hz with laser pulse energies of  $\sim 10 \mu\text{J}/\text{pulse}$ . The OPO beam ( $\sim 1 \text{ mJ}/\text{pulse}$  delivered to the chamber) is spatially overlapped with the dye laser and precedes it in time by about 100 ns. When the infrared radiation is resonant with a transition out of the same ground-state level as probed by the monitor transition, population is removed from this level and is detected as a dip in the fluorescence.

Given the large fluorescence signals possible in these experiments ( $10^5$  photons/pulse), shot noise limitations on the detectable depletions are quite small (0.3%). As a result, the major noise sources present in the experiment are due to dye laser power fluctuations and fluctuations in the pulsed valve. Rather than employing a dual beam scheme for such corrections (as we have implemented in RIDIR spectroscopy) in the present case such fluctuations are corrected for by using two boxcar averagers, both operating in the active baseline subtraction mode.<sup>12</sup> In the limit of linear fluorescence signal, an ideal power-normalized fluorescence-dip signal will be

$$(S_i - NP_i) - (S_j - NP_j),$$

where  $S_i$  and  $S_j$  are fluorescence signals from two successive dye laser pulses, one with the OPO on, the other with it off.  $P_i$  and  $P_j$  are the laser power photodiode signals for these pulses, and  $N$  is a scaling factor relating the magnitudes of the fluorescence and laser power signals, chosen so that in the absence of the OPO,  $(S_i - NP_i) = 0$ .

Precisely this form can be achieved in hardware by using two boxcar averagers, (one for signal, and the other for laser power) in the active baseline subtraction mode, i.e.,

$$\text{FDIR signal} = (S_i - S_j) - N(P_i - P_j),$$

where the value for  $N$  is chosen after-the-fact in software. Perhaps the greatest advantage of this method is that it very effectively corrects for any long-term fluctuations in the fluorescence and laser power signals. Since in the present case, several of the absorptions are broad and weak, the elimination of spurious bumps in the spectrum is an important factor in the experiment. With this method, depletions of a few percent can be observed after only modest signal averaging (50–100 laser shots per data point).

The wavelength calibration of the OPO is obtained by recording the photoacoustic absorption spectrum of room temperature methane and water.

### III. DENSITY FUNCTIONAL THEORY CALCULATIONS ON TROPOLONE AND TROPOLONE-OD

Previous computational studies have used Hartree–Fock<sup>1(c)</sup> and Møller–Plesset perturbation theory at the MP2 level<sup>13</sup> to calculate the minimum-energy structure, vibrational frequencies, and H-atom tunneling transition state properties of tropolone. Here we apply density functional theory (DFT) methods to tropolone, both for comparison of

the method with the previous calculations, and to provide seamless comparison with the DFT calculations on the tropolone-H<sub>2</sub>O complex reported in the following paper. The DFT calculations employ the Becke3LYP nonlocal exchange–correlation functional<sup>27,28</sup> which has been found to provide results of comparable accuracy to MP2 calculations with the same basis set for both water clusters and benzene-(H<sub>2</sub>O)<sub>*n*</sub> clusters.<sup>29</sup> In the Becke3LYP procedure, the energy contains contributions from local and nonlocal exchange and correlation functionals<sup>28</sup> as well as from the exact exchange.

Two different basis sets,<sup>30</sup> 6-31+G\* and 6-31+G'[2*d*,*p*], were used, the former for survey calculations and the latter for more accurate calculations. In both cases, five-component *d* functions were employed. The 6-31+G'[2*d*,*p*] basis set combines the standard 6-31+G(2*d*,*p*) basis set for the carbon atoms and the 6-31+G[2*d*,*p*] basis set for the O and H atoms. The 6-31+G[2*d*,*p*] basis set is formed by combining the 6-31+G(2*d*,*p*) basis set with polarization functions from the aug-cc-pVDZ basis set, and has been used previously in studies of water clusters and benzene-(H<sub>2</sub>O)<sub>*n*</sub> clusters.<sup>29</sup> For these species, Becke3LYP and MP2 calculations with the 6-31+G[2*d*,*p*] basis set have been found to give structures, vibrational frequency shifts, and infrared intensities in good agreement with experiment.

Table I lists the key structural parameters for TrOH using the DFT methods. In Table II, the infrared frequencies, intensities, and approximate normal mode descriptions are given for TrOH using both the 6-31+G\* and 6-31+G'[2*d*,*p*] basis sets and for TrOD using the 6-31+G'[2*d*,*p*] basis set.

### IV. EXPERIMENTAL RESULTS AND ANALYSIS

Figure 3 presents the fluorescence excitation spectrum of the  $S_1 \leftarrow S_0$  origin tunneling doublet used to monitor population in the lower [ $0_0^0(a_1'')$ ] and upper [ $0_0^0(b_2'')$ ] members of tropolone's ground-state tunneling doublet. The double prime (") attached to the symmetry designations denotes the OH( $v=0$ ) tunneling levels while a single prime (') is used for the OH( $v=1$ ) tunneling levels. The tunneling splitting at the zero-point level of the ground-state is known from microwave studies<sup>31</sup> to be  $0.99 \text{ cm}^{-1}$ . Hence, both  $a_1''$  and  $b_2''$  levels have significant population even at the low temperatures present in the supersonic free jet. The increase in the tunneling splitting at the  $S_1$  origin to  $19 \text{ cm}^{-1}$  provides the means for recording infrared spectra in FDIRS out of the lower ( $a_1''$ ) or upper ( $b_2''$ ) members of the ground-state tunneling doublet free from interference from one another. In a sense, the FDIR spectra are "symmetry labeled" in that they are known to arise exclusively from a single tunneling level of definite symmetry.

FDIR spectra out of the  $a_1''$  and  $b_2''$  levels of TrOH are shown in Figs. 4(a) and 4(b), respectively. The two spectra are surprisingly similar given the expectation that a quartet of absorptions due to the O–H stretch fundamental should be

TABLE I. Key bond lengths  $r$  (Å) and bond angles  $a$  (degrees) of tropolone at the indicated levels of theory.

	Becke3LYP 6-31+G*	Becke3LYP 6-31+G'[2d,p]	MP2 6-31+G'[2d,p]
$r$ C <sub>1</sub> -C <sub>2</sub>	1.485	1.483	1.471
$r$ C <sub>2</sub> -C <sub>3</sub>	1.379	1.377	1.389
$r$ C <sub>3</sub> -C <sub>4</sub>	1.413	1.411	1.408
$r$ C <sub>4</sub> -C <sub>5</sub>	1.380	1.378	1.389
$r$ C <sub>5</sub> -C <sub>6</sub>	1.417	1.415	1.414
$r$ C <sub>6</sub> -C <sub>7</sub>	1.377	1.375	1.384
$r$ C <sub>7</sub> -C <sub>1</sub>	1.438	1.435	1.438
$r$ C <sub>1</sub> -O <sub>1</sub>	1.254	1.249	1.260
$r$ C <sub>2</sub> -O <sub>2</sub>	1.337	1.330	1.337
$r$ O <sub>2</sub> -H <sub>2</sub>	0.995	0.993	0.995
$r$ O <sub>1</sub> -O <sub>2</sub>	2.507	2.486	2.501
$r$ O <sub>1</sub> -H <sub>2</sub>	1.828	1.789	1.795
$r$ C <sub>3</sub> -H	1.088	1.088	1.090
$r$ C <sub>4</sub> -H	1.088	1.089	1.090
$r$ C <sub>5</sub> -H	1.087	1.088	1.089
$r$ C <sub>6</sub> -H	1.089	1.090	1.091
$r$ C <sub>7</sub> -H	1.088	1.088	1.091
$a$ C <sub>1</sub> -C <sub>2</sub> -C <sub>3</sub>	130.1	130.0	130.3
$a$ C <sub>2</sub> -C <sub>3</sub> -C <sub>4</sub>	129.0	129.0	129.0
$a$ C <sub>3</sub> -C <sub>4</sub> -C <sub>5</sub>	129.4	129.4	129.0
$a$ C <sub>4</sub> -C <sub>5</sub> -C <sub>6</sub>	127.5	127.5	127.7
$a$ C <sub>5</sub> -C <sub>6</sub> -C <sub>7</sub>	130.3	130.3	130.0
$a$ C <sub>6</sub> -C <sub>7</sub> -C <sub>1</sub>	130.4	130.3	130.7
$a$ C <sub>7</sub> -C <sub>1</sub> -C <sub>2</sub>	123.3	123.4	123.1
$a$ C <sub>2</sub> -C <sub>1</sub> -O <sub>1</sub>	114.8	114.6	115.1
$a$ C <sub>1</sub> -C <sub>2</sub> -O <sub>2</sub>	111.6	111.2	111.6
$a$ C <sub>2</sub> -O <sub>2</sub> -H <sub>2</sub>	103.9	103.0	102.1
$a$ O <sub>2</sub> -H <sub>2</sub> -O <sub>1</sub>	122.4	124.1	124.8
$a$ C <sub>2</sub> -C <sub>3</sub> -H	114.4	114.5	113.9
$a$ C <sub>3</sub> -C <sub>4</sub> -H	114.6	114.6	115.1
$a$ C <sub>4</sub> -C <sub>5</sub> -H	116.6	116.6	116.3
$a$ C <sub>5</sub> -C <sub>6</sub> -H	114.8	114.8	115.2
$a$ C <sub>6</sub> -C <sub>7</sub> -H	117.2	117.3	116.9

present in this region. The interpretation of the spectrum is complicated by the proximity of the C–H stretch and O–H stretch absorptions in tropolone. As is evident from Table II, the calculations predict a set of five C–H stretch fundamentals all of which carry some intensity. The calculated frequencies separate into two groups, a set of two separated to lower frequency by about 30 cm<sup>-1</sup> from the other three. After shifting the calculated frequencies to match up the lowest-frequency calculated (3147 cm<sup>-1</sup>) and experimental C–H stretch bands (3034 cm<sup>-1</sup>), the correspondence with experiment suggests that the bands at 3034 and 3040 cm<sup>-1</sup> are the lower frequency set of two C–H stretches, and the partially resolved set of bands centered at 3071 cm<sup>-1</sup> are the three higher frequency C–H stretches. Such an assignment is in keeping with the room temperature gas-phase infrared assignment<sup>3</sup> of two peaks at 3030 and 3055 cm<sup>-1</sup> to the C–H stretch modes. Of course, Fermi resonance mixing with overtones or combination bands (e.g., CC stretch or CH bend) may effect the positions and intensities of the observed bands. Nevertheless, the assignment of the bands below 3100 cm<sup>-1</sup> as CH stretch leaves the other transitions peaked at 3134 cm<sup>-1</sup> in Figs. 4(a) and 4(b) as O–H stretch absorptions.

In order to test this assignment, the FDIR spectrum of

TrOD was recorded over the same spectral region as previously. With the present OPO, the O–D stretch of TrOD cannot be directly probed, since it is at too low a frequency (~2300 cm<sup>-1</sup>). Nevertheless, the spectrum of TrOD in the O–H and C–H stretch region can highlight the O–H stretch absorptions in TrOH through the transition(s) that disappear from the spectrum.

The FDIR spectrum of TrOD is shown in Fig. 5(a), with the TrOH(*a*<sub>1</sub>) spectrum shown below it for direct comparison. Due to the smaller tunneling splitting in the *S*<sub>1</sub>←*S*<sub>0</sub> spectrum of TrOD, the FDIR spectrum of Fig. 5(a) includes contributions from both the *a*<sub>1</sub> and *b*<sub>2</sub> ground-state levels due to partial overlap of the bands in the electronic spectrum. As anticipated, the main band at 3134 cm<sup>-1</sup> is gone from the TrOD spectrum, though a weak feature at 3105 cm<sup>-1</sup> remains. The set of C–H stretch bands at 3034 and 3070 cm<sup>-1</sup> is virtually unchanged.

The assignment of the 3105 cm<sup>-1</sup> band of TrOD [Fig. 5(a)] is not clear. It may be a dark background state in Fermi resonance with the C–H stretch, or an overtone or combination band carrying its own oscillator strength. As is evident from Table II and from the experimental data of Ikegami<sup>3</sup> and Redington,<sup>2</sup> several strongly absorbing infrared bands occur in the 1500–1600 cm<sup>-1</sup> region, and overtones or combinations of these bands are of roughly the right frequency to produce the 3105 cm<sup>-1</sup> band.

The comparison of the spectra of TrOD with TrOH provides strong evidence that the 3134.9 and 3133.9 cm<sup>-1</sup> bands in Figs. 4(a) and 4(b), respectively, are due to the O–H stretch. Confirming evidence for this assignment comes from two sources. First, our expectation from the energy level diagram of Fig. 1 is that each transition in the *a*<sub>1</sub> spectrum will be mirrored by a transition of opposite polarization (*y*↔*z*) out of the upper tunneling level (*b*<sub>2</sub> symmetry), and that the corresponding transitions out of the *b*<sub>2</sub> state will differ in frequency from those in the *a*<sub>1</sub> spectrum by the ground state tunneling splitting of 0.99 cm<sup>-1</sup>. The observed frequency difference between the two bands is of this magnitude (1.0 ± 0.4 cm<sup>-1</sup>), in fortuitously close agreement with the prediction. Given the OPO bandwidth, a splitting of this magnitude is difficult to quantify. Nevertheless, the difference in peak frequencies is known to considerably better accuracy than either absolute frequency, depending only on the repeatability of the scanning of the OPO. Based on this assignment, the 3134.9 and 3133.9 cm<sup>-1</sup> bands originate from the lower and upper zero-point tunneling states (Fig. 1) and terminate in the same OH(*v* = 1) tunneling level. Second, the tentative assignment of the OH stretch in the room temperature infrared spectrum of Ikegami<sup>3</sup> was to a band at 3140 cm<sup>-1</sup>, very close to the two bands observed here.

Despite the considerable support for the assignment just given for the 3133.9 and 3134.9 cm<sup>-1</sup> transitions, other features of the spectrum are less well understood. First, one must explain the remarkable similarity of the *a*<sub>1</sub> and *b*<sub>2</sub> level spectra, and in particular the reason that the 3133.9 and 3134.9 cm<sup>-1</sup> transitions are so similar in intensity in the two spectra (relative to the C–H stretch bands) despite being of different polarization. Second, the transitions to the other

TABLE II. Infrared frequencies and intensities for TrOH using both the 6-31+G\* and 6-31+G'[2*d,p*] basis sets and for TrOD using the 6-31+G'[2*d,p*] basis set.

TrOH <sup>a</sup>				TrOD <sup>b</sup>	
Becke3LYP/6-31+G*		Becke3LYP/6-31+G'[2 <i>d,p</i> ]		Becke3LYP/6-31+G'[2 <i>d,p</i> ]	
Frequency (in cm <sup>-1</sup> )	Intensity (in km/mol)	Frequency (in cm <sup>-1</sup> )	Intensity (in km/mol)	Frequency (in cm <sup>-1</sup> )	Intensity (in km/mol)
114.9	1.1	120.6	1.0	120.5	1.0
185.1	0.0	183.8	0.0	182.4	0.0
363.4	6.1	358.6	10.1	341.6	13.3
373.9	4.8	370.4	2.7	368.2	1.5
376.1	0.0	377.8	0.0	377.6	0.0
402.2	1.8	403.9	2.1	401.4	3.1
448.4	15.0	445.6	15.2	439.2	13.3
545.9	1.8	549.8	1.9	547.1	2.0
597.6	0.2	601.9	0.1	598.3	3.5
694.2	7.3	693.8	6.5	692.8	6.6
724.8	19.6	739.5	33.5	740.7	50.2
751.5	14.3	751.9	14.5	748.3	12.2
773.2	79.7	783.0	51.5	785.6	26.2
814.8	76.7	849.7	58.1	622.3	35.2
878.4	10.3	885.1	10.1	882.8	1.2
888.4	10.8	885.3	10.5	884.2	7.4
945.0	11.2	941.7	11.6	941.7	11.9
977.5	10.3	973.2	9.9	964.5	35.4
1014.2	0.3	1012.3	0.2	1012.3	0.3
1030.2	1.1	1028.8	1.1	1028.8	0.8
1080.6	0.4	1077.1	0.4	1000.7 <sup>c</sup>	22.2
1244.6	7.8	1236.8	4.5	1238.9	4.2
1248.9	7.5	1241.9	7.3	1257.2 <sup>c</sup>	77.6
1294.1	44.8	1282.3	32.0	1290.0	32.3
1324.9	223.5	1320.7	203.1	1117.4 <sup>c</sup>	41.7
1349.0	61.3	1343.7	63.7	1341.4	123.4
1454.6	25.5	1442.2	19.0	1442.5	40.9
1479.8	211.8	1470.2	212.4	1432.5	66.0
1523.9	139.4	1515.3	144.4	1511.8	70.9
1540.4	116.5	1533.9	133.8	1525.9	83.6
1618.6	108.1	1612.0	91.9	1602.6	196.0
1664.7	1.6	1655.6	8.5	1652.8	11.3
1675.2	208.7	1672.6	202.7	1663.9	233.1
3163.0	6.4	3147.3	5.7	3147.3	5.7
3172.0	3.7	3156.2	2.9	3156.3	2.5
3186.3	12.2	3171.7	7.7	3171.7	7.7
3193.2	15.2	3176.9	9.7	3176.9	10.0
3198.2	8.3	3184.1	8.2	3184.1	8.3
3331.6	132.8	3337.3	143.5	2427.4	87.0

<sup>a</sup>The modes in TrOH are listed in order of increasing frequency.

<sup>b</sup>The modes in TrOD are listed in an order which provides one-to-one correspondence with the analogous modes in TrOH.

<sup>c</sup>These modes in TrOD are mixtures of several modes in TrOH.

OH( $\nu = 1$ ) tunneling level are not obviously apparent nor easily assigned. As shown in Fig. 6, in TrOH( $a_1$ ), we have carefully searched the entire region from 2700 to 3450 cm<sup>-1</sup> for transitions ascribable to the other OH( $\nu = 1$ ) tunneling level. This has met without success, despite a signal-to-noise level sufficient to observe sharp transitions ten times less intense than the 3135 cm<sup>-1</sup> band.

In the discussion section, we will take up these unresolved issues in the context of a simple model for tunneling in tropolone in the high barrier limit.

## V. DISCUSSION

### A. Comparison of experiment with the predictions for TrOH tunneling in the high barrier limit

In this section, a simple model for the OH stretch band intensities is presented which assumes that the barrier to H-atom tunneling is high enough that the OH stretch vibrational wave functions are largely localized around the two minima in the potential energy surface. A primary test of the model is whether it can successfully account for the similar

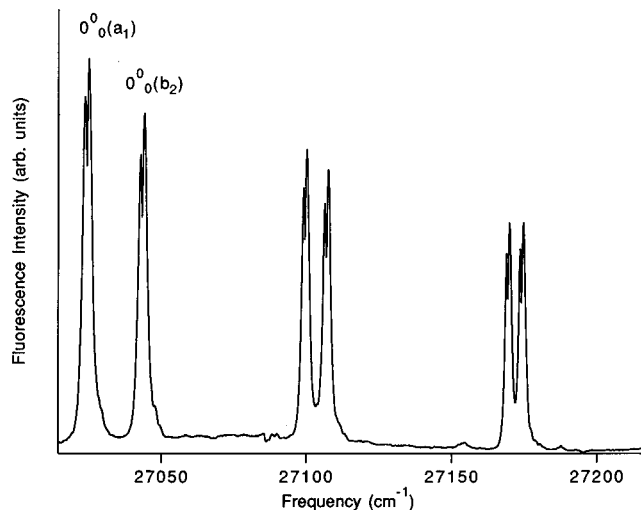


FIG. 3. Fluorescence excitation spectrum of the  $S_1 \leftarrow S_0$  origin region of TrOH. The  $0^0_0(a_1')$  and  $0^0_0(b_2')$  transitions are used to monitor the lower and upper zero-point tunneling levels in the fluorescence-dip infrared spectroscopy.

experimental intensities of the 3133.9 and 3134.9  $\text{cm}^{-1}$  transitions. The OH stretch  $v=0$  and  $v=1$  wave functions are written as simple sums and differences of wave functions localized in the right- ( $|Rn\rangle$ ) and left-hand wells ( $|Ln\rangle$ ), i.e.,

$$|a_1''\rangle = \frac{1}{\sqrt{2}} (|L0\rangle + |R0\rangle),$$

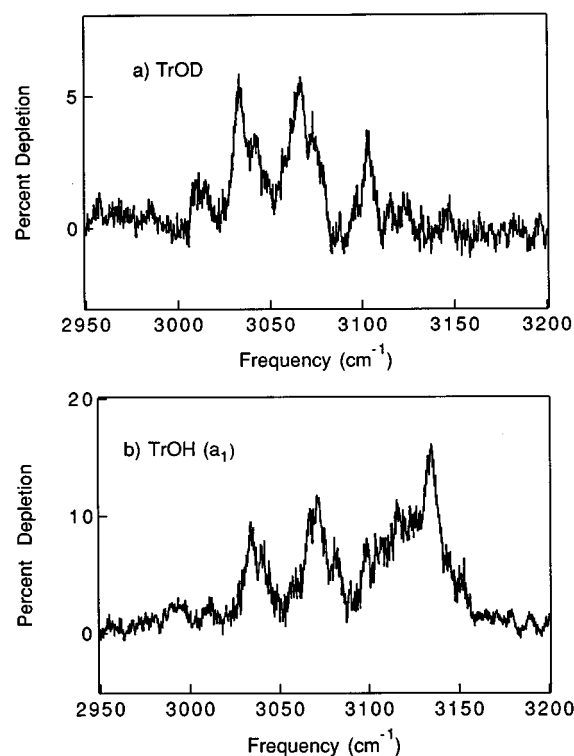


FIG. 5. FDIR spectra of (a) tropolone deuterated in the hydroxy position (TrOD), and (b) TrOH( $a_1'$ ) for comparison.

$$|b_2''\rangle = \frac{1}{\sqrt{2}} (|L0\rangle - |R0\rangle),$$

$$|a_1'\rangle = \frac{1}{\sqrt{2}} (|L1\rangle + |R1\rangle),$$

$$|b_2'\rangle = \frac{1}{\sqrt{2}} (|L1\rangle - |R1\rangle).$$

(2)

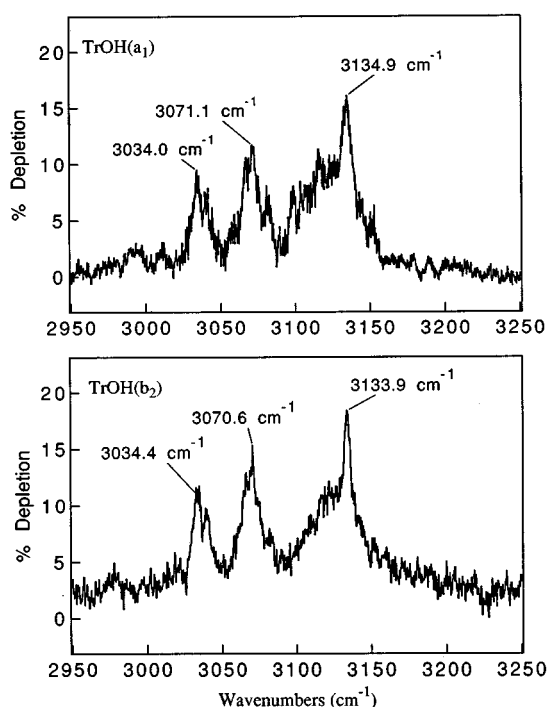


FIG. 4. FDIR spectra out of the  $a_1'$  and  $b_2'$  levels of TrOH.

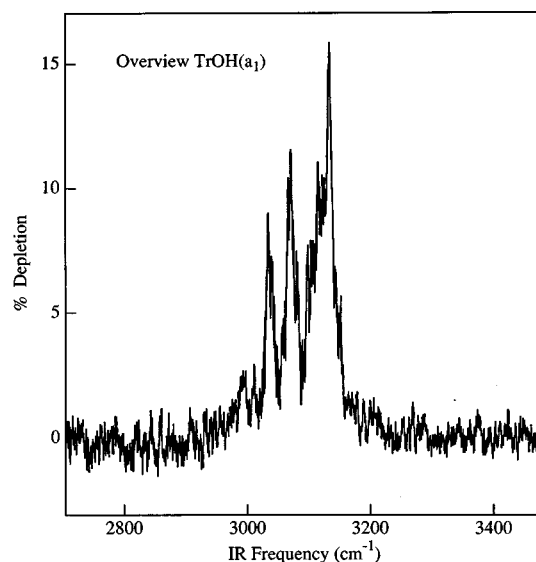


FIG. 6. Overview FDIR spectrum used in searching for the other member of the OH( $v=1$ ) tunneling doublet in the TrOH( $a_1'$ ) spectrum.

Here the  $G_4$  symmetry designations for the OH stretch levels are those in Fig. 1 where H-atom tunneling is feasible. The single (double) prime refers to the  $v=0$  ( $v=1$ ) tunneling levels. In order to approximate the  $y$ - and  $z$ -polarized OH stretch band intensities, the  $y$  and  $z$  components of the dipole moment function are expanded about the two equilibrium positions, one in the right-hand and one in the left-hand well:

$$\mu_y = \mu_{e,y} + \left[ \left( \frac{\partial \mu_y}{\partial Q_L} \right)_e Q_L - \left( \frac{\partial \mu_y}{\partial Q_R} \right)_e Q_R \right]$$

and

$$\mu_z = \mu_{e,z} + \left[ \left( \frac{\partial \mu_z}{\partial Q_L} \right)_e Q_L + \left( \frac{\partial \mu_z}{\partial Q_R} \right)_e Q_R \right]. \quad (3)$$

The form of the terms in brackets produces a nonzero dipole moment derivative along either the  $y$  or  $z$  axes, respectively. The intensity of the four OH stretch ( $v=0-1$ ) transitions is then given by

$$\begin{aligned} I(a_1'' \rightarrow a_1') &= \left| \left( \frac{\partial \mu_z}{\partial Q_L} \right) \langle a_1'' | [Q_L + Q_R] | a_1' \rangle \right|^2, \\ I(b_2'' \rightarrow b_2') &= \left| \left( \frac{\partial \mu_z}{\partial Q_L} \right) \langle b_2'' | [Q_L + Q_R] | b_2' \rangle \right|^2, \\ I(a_1'' \rightarrow b_2') &= \left| \left( \frac{\partial \mu_y}{\partial Q_L} \right) \langle a_1'' | [Q_L - Q_R] | b_2' \rangle \right|^2, \\ I(b_2'' \rightarrow a_1') &= \left| \left( \frac{\partial \mu_y}{\partial Q_L} \right) \langle b_2'' | [Q_L - Q_R] | a_1' \rangle \right|^2, \end{aligned} \quad (4)$$

where we have made use of the fact that  $|(\partial \mu_y / \partial Q_R)| = |(\partial \mu_y / \partial Q_L)|$ . If the barrier to tunneling is quite high, we can assume negligible overlap between the wave functions in the left-hand and right-hand wells even in the OH( $v=1$ ) state. This assumption has some basis in the approximately correct CH stretch/OH stretch intensity ratio predicted by the *ab initio* calculation, which is inherently a small-amplitude calculation. In this limit, the ratio of intensities of the  $y$ - and  $z$ -polarized transitions is just

$$\frac{I(y)}{I(z)} = \left( \frac{\partial \mu_y / \partial Q_L}{\partial \mu_z / \partial Q_L} \right)^2. \quad (5)$$

The magnitude of the  $y$  and  $z$  components of the dipole moment derivatives are determined from a series of single point calculations of the dipole moment as a function of displacement along the OH stretch normal mode. The slope of this plot was very nearly linear over a range of OH bond lengths bounded by the classical turning points at the zero-point level. The calculation yields a value of 1.18 for the  $[(\partial \mu_y / \partial Q_L) / (\partial \mu_z / \partial Q_L)]$  ratio, in close correspondence with the ratio of projections of the OH stretch normal mode onto the  $y$  and  $z$  axes. Substituting this ratio into Eq. (5) yields a ratio of  $y$ - to  $z$ -polarized transition intensities of 1.4, a value close enough to 1.0 to account satisfactorily for the similar intensities of the 3133.9 and 3134.9  $\text{cm}^{-1}$  bands in the experimental spectra.

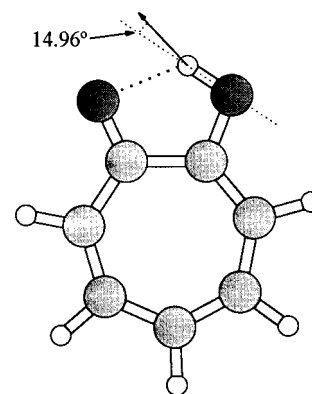


FIG. 7. The OH stretch normal mode calculated at the Becke3LYP/6-31+G\*[2d,p] level of theory. Note the  $15^\circ$  rotation of the displacement vector from the OH bond axis.

The qualitative form of the spectrum predicted by this model is shown in Fig. 1. The intensity ratio is close to 1.0 partly because the OH stretch mode does not oscillate directly along the OH bond axis, but at an angle of  $15^\circ$  to it, as shown in Fig. 7. This is a consequence of the highly nonlinear H bond in TrOH in which the O–O separation is only 2.50 Å. It would appear that the OH is riding up against the keto oxygen in such a way that as it stretches, it is forced away from the keto oxygen. This effectively introduces a component of OH bend to the normal mode, and more nearly equalizes the  $y$  and  $z$  components of the hydrogen's motion.

As shown in Fig. 1, the prediction of the model is that the FDIR spectra out of the  $a_1''$  and  $b_2''$  levels should each support another transition of comparable intensity to the 3133.9 and 3134.9  $\text{cm}^{-1}$  transitions, yet no such transitions are readily apparent. Several possible explanations can be given. First, the OH( $v=1$ ) tunneling splitting could be small enough that the other transitions are unresolved. This would seem unlikely given the zero-point level tunneling splitting of 1.0  $\text{cm}^{-1}$  in TrOH and the neon matrix data<sup>2</sup> on TrOD which gives a 19  $\text{cm}^{-1}$  splitting for OD( $v=1$ ). This latter value is likely influenced by matrix effects, but is nevertheless qualitatively larger than that required for resolution in our spectra. Second, the other transitions may be obscured by the C–H stretch bands. To test this possibility clearly, FDIR spectra of  $\text{C}_7\text{D}_5\text{OH}$  will need to be taken in the future. Third, the comparison between the TrOH and TrOD spectra (Fig. 5) suggests that at least part of the intensity in the broad shoulder to the low-frequency side of the 3133.9 and 3134.9  $\text{cm}^{-1}$  bands is due to the OH stretch, and could be ascribed to transitions to the other tunneling level. This seems the most likely possibility at present. If true, it would mean that the 3133.9 and 3134.9  $\text{cm}^{-1}$  transitions terminate in the  $b_2'$  level, and that the  $a_1'$  level is broadened by state mixing with background states.

Assuming that the entire broad shoulder can be ascribed to the transition to the  $a_1'$  level, the TrOH( $b_2''$ ) 3100–3150  $\text{cm}^{-1}$  region has been fit as the sum of two Gaussians. A reasonable fit to the spectrum in this region is achieved with Gaussians centered at 3122 and 3133.9  $\text{cm}^{-1}$ , giving a 12

$\text{cm}^{-1}$  OH( $v=1$ ) splitting. The full-widths of the Gaussians are 30 and  $4 \text{ cm}^{-1}$ , respectively, while the relative intensities of the bands are  $I_{\text{shoulder}}/I_{3134} \approx 5$ , a value significantly greater than that predicted by our simple model (1.4). Thus, the data is suggestive but not definitive in its support of the assignment of the broad shoulder as the transition to the other member of the OH( $v=1$ ) tunneling doublet.

Recently, Smedarchina *et al.*<sup>32</sup> reported results of a full multidimensional instanton calculation of vibrationally mode-specific tunneling splittings in tropolone. This promising approach yields  $S_1$  tunneling splittings which for totally symmetric modes match experimental observations to remarkable accuracy. When applied to the  $S_0$  OH( $v=1$ ) level,<sup>33</sup> the calculated tunneling splittings are  $15.5/0.8 \text{ cm}^{-1}$  for TrOH/TrOD using their model potential, and  $12.9/0.7 \text{ cm}^{-1}$  with a numerical potential. The close correspondence with the  $12 \text{ cm}^{-1}$  splitting suggested above provides confirming evidence for the proposed assignment.

Regarding the breadths of the bands, it is not surprising that significant state mixing is present in tropolone at this energy. Elegant experiments<sup>34–40</sup> employing high-resolution spectroscopy and/or multiresonant excitation have provided a detailed picture of state mixing in hydride stretch fundamentals and overtones of molecules of widely varying complexity. Even within the more restrictive category of aromatics, the coupling is seen to range over several orders-of-magnitude. In naphthalene, the C–H stretch fundamental is coupled with background states with an average coupling matrix element of only  $0.0016 \text{ cm}^{-1}$ . In pyrazine, the analogous coupling bears a coupling matrix element of  $0.36 \text{ cm}^{-1}$ , while in benzene and fluorobenzene, coupling matrix elements of the C–H stretch with the overtones and combinations of the ring CC stretch vibrations are of order  $10 \text{ cm}^{-1}$ . In TrOH, the large number of vibrational modes (39), the relative floppiness of the ring, the presence of several potential 2–1 Fermi resonances, and the large-amplitude H-atom tunneling motion all might suggest that state mixing in OH (and CH)  $v=1$  would be large.

What is perhaps more surprising, in light of the tentative OH stretch assignments given, is the mode-specific nature of the state mixing. Accepting the assignment of the broad shoulders at  $3120 \text{ cm}^{-1}$  (Fig. 4) as OH stretch transitions terminating in the  $a'_1$  level (Fig. 1) necessitates coupling matrix elements for  $a'_1$  and  $b'_2$  OH stretch ( $v=1$ ) levels with the background states which differ by about an order-of-magnitude. The source of these differences will need to be explored further if the assignments of the  $a'_1 \leftarrow a''_1$  and  $a'_1 \leftarrow b''_2$  transitions stand up to future tests.

## B. Tropolone and its intramolecular hydrogen bond

One of the anomalies of the IR spectrum of tropolone is that the large frequency shift of the OH stretch is accompanied by no corresponding intensity increase of the OH stretch infrared absorption. In intermolecularly hydrogen-bonded systems, the strength of the hydrogen bond is correlated with three features of the X–H stretch infrared absorption: the magnitude of the frequency shift, the integrated absorption intensity, and the breadth of the transition.<sup>24</sup> In these sys-

tems, the formation of the hydrogen bond both lowers the frequency of the OH stretch and enhances the dipole moment derivative ( $\partial\mu/\partial Q_{\text{OH}}$ ) which determines the infrared intensity. This enhancement can lead to OH stretch intensity increases of a factor of 5 or more over the unhydrogen-bonded intensity. For example, in the phenol– $\text{H}_2\text{O}$  complex, the hydrogen-bonded OH stretch is six times more intense than the free OH in phenol monomer.<sup>21(c)</sup>

In the case of tropolone, the frequency shift of the observed OH stretch absorption ( $3134 \text{ cm}^{-1}$ ) relative to a typical free OH stretch absorption ( $\sim 3710 \text{ cm}^{-1}$ ) is about  $580 \text{ cm}^{-1}$ , extremely large for an  $\text{O}\cdots\text{HO}$  hydrogen bond. At the same time, the experimental intensity is only about two to three times the total integrated intensity of the C–H stretching modes. In keeping with this, the *ab initio* calculation (Table II) predicts a tropolone OH stretch intensity four times the total intensity of the five C–H stretch absorptions and less than a factor of 2 larger than that of a free OH (using the same basis set).

The large frequency shift and small intensity of intramolecularly H-bonded OH stretch vibrations has been the subject of previous studies in the condensed phase.<sup>2,24,25</sup> Here we comment on this issue from the perspective of the cold, isolated molecule. One suggestion which has been made is that the intensity weakness is a consequence of the delocalization of the OH( $v=1$ ) levels due to facile tunneling in those levels.<sup>2</sup> However, as we will see in the adjoining paper, the intensity of the TrOH OH stretch remains relatively constant in going from TrOH to TrOH– $\text{H}_2\text{O}$ , despite the localization which accompanies the asymmetrization of the double minimum well upon complexation of water. Furthermore, the qualitative intensity trends are correctly reproduced by the *ab initio* calculations, which are inherently small-amplitude harmonic calculations. Thus, one is inclined to look for explanations for the large frequency shift and small intensity increase which are independent of the tunneling process, and more generally characteristic of intramolecular H bonds.

The intramolecular H bond of tropolone is atypical in that it is strongly bent, with the O–H bond at a  $38^\circ$  angle relative to a line joining the oxygen atoms. At the same time, the O–O separation in TrOH is only  $2.50 \text{ \AA}$  (Table I), much shorter than a typical  $\text{O–H}\cdots\text{O}$  intermolecular H bond ( $2.98 \text{ \AA}$  in the water dimer).<sup>17</sup> The results of a series of calculations designed to test the effect of the intramolecular H bond on the OH stretch vibrational frequencies and intensities are summarized in Table III. The table draws a first comparison between the structures and OH stretch infrared spectra of *cis*-tropolone (i.e., in its minimum energy intramolecularly H-bonded configuration) with *trans*-tropolone, the secondary minimum structure in which the OH bond points away from the keto oxygen in a non H-bonded configuration. From a structural viewpoint, the intramolecular H bond lengthens the OH bond ( $\Delta r_{\text{OH}} = .024 \text{ \AA}$ ), draws the two oxygens .061  $\text{ \AA}$  closer together, and bends the OH bond toward the keto oxygen ( $\Delta\theta_{\text{COH}} = 103.9^\circ - 110.2^\circ = -6.3^\circ$ ). As expected, the spectral consequences of the intramolecular H bond are a large decrease in the OH stretch frequency (by  $355 \text{ cm}^{-1}$ ), but an

TABLE III. Key calculated spectroscopic and structural parameters of *cis* and *trans* TrOH, TrOH-H<sub>2</sub>O,<sup>a</sup> and *cis* and *trans* hydroxyacetaldehyde (HOAA) calculated at the Becke3LYP/6-31+G\* level of theory.

	Frequency (in cm <sup>-1</sup> )	Frequency shift relative to H <sub>2</sub> O <sup>b</sup> (in cm <sup>-1</sup> )	Frequency shift relative to <i>trans</i> species (in cm <sup>-1</sup> )	Intensity (in km/mol)	$r_{\text{O}\cdots\text{H}}$ (Å)	$r_{\text{O}-\text{O}}$ (Å)	$\alpha_{\text{O}-\text{O}\cdots\text{H}}$ (deg)	$\alpha_{\text{C}\cdots\text{O}\cdots\text{H}}$ (deg)
<i>cis</i> TrOH	3331.6	-457.5	-391.9	132.8	0.995	2.507	38.0	103.9
<i>trans</i> TrOH	3723.5	-65.5	0.0	65.6	0.972	2.568	N/A	110.2
	3368.0	-421.0	-355.4	165.2				
TrOH·H <sub>2</sub> O <sup>a</sup>	3556.7	-232.3	-166.8	607.1	0.993	2.502	N/A	104.2
	3825.2	36.2	101.7	106.9				
<i>cis</i> HOAA	3640.9	-148.1	-120.2	60.6	0.977	2.706	45.3	107.1
<i>trans</i> HOAA	3761.2	-27.9	0.0	40.0	0.969	2.745	N/A	109.1

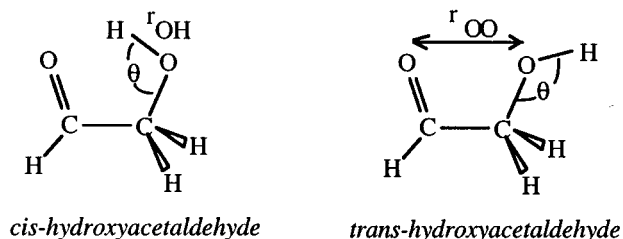
<sup>a</sup>Conformational isomer with water hydrogen bonded to the exterior side of the keto-oxygen on tropolone.

<sup>b</sup>The shift is reported relative to the average of the symmetric and asymmetric OH stretches in H<sub>2</sub>O calculated at the same level of theory.

OH stretch intensity increase of only about a factor of 2.

The tropolone-H<sub>2</sub>O complex provides a second comparison. As we shall show in more detail in the succeeding paper, there are several structural conformers calculated for tropolone-H<sub>2</sub>O. One of these, the “exterior” isomer, the water acts as hydrogen donor to the exterior side of the keto oxygen, leaving the intramolecular H bond of tropolone relatively undisturbed. As a result, the exterior isomer incorporates a free OH, an intermolecular OH⋯O=C hydrogen bond, and an intramolecular OH⋯O=C hydrogen bond in the same complex, facilitating direct comparison between the three types of OH groups. As seen in Table III, the frequency shift of the OH involved in an intermolecular H bond is almost a factor of 2 smaller than the intramolecularly H-bonded OH, yet the intensity of the former is almost four times the latter.

Finally, we have tested the generality of the effects of intramolecular H-bond formation on the OH stretch absorption by carrying out calculations on hydroxyacetaldehyde (HOAA), shown below. Experimentally, the OH stretch fundamental in HOAA is at 3549 cm<sup>-1</sup>, almost 400 cm<sup>-1</sup> less red shifted than in tropolone.<sup>41</sup> It is thus of interest to see the structural and spectroscopic changes computed for HOAA by comparison to tropolone.



In HOAA, the unconjugated C-C single bond joining the keto and OH groups lengthens the O-O separation,  $r_{\text{OO}}$ , to 2.706 Å, suggesting a weaker intramolecular H bond than in TrOH. Consistent with this conclusion, the OH bond length (0.977 Å) in HOAA is significantly shorter than in TrOH (0.995 Å). Furthermore, the structural differences between *cis* (H-bonded OH) and *trans* (free OH) forms of HOAA are also significantly less than the analogous differences in TrOH, most notably in the change in the OH bond

length ( $\Delta r_{\text{OH}} = +0.008$  Å), O-O separation ( $\Delta r_{\text{OO}} = -0.039$  Å), and COH bond angle ( $\Delta \theta_{\text{COH}} = -2.9^\circ$ ) upon H-bond formation. In keeping with experiment, the *ab initio* calculation predicts that the OH stretch frequency shift between the H-bonded *cis* and unhydrogen-bonded *trans* forms is only 120 cm<sup>-1</sup>, while the intensity increase so produced is only 1.5 times.

One surmises based on the calculations on TrOH, TrOH-H<sub>2</sub>O, and HOAA that the OH stretch intensity in a bent intramolecular H bond is a weak function of the O-O separation, while the OH stretch frequency depends very sensitively on this distance. Whether it is the frequency shift or the lack of intensity increase which is unusual by comparison to intermolecular hydrogen bonds is still an open question.

## VI. CONCLUSION

FDIR spectroscopy has been used to record near-infrared spectra of tropolone out of the lower and upper levels of the H-atom tunneling doublet free from interference from one another. Assignments of two of the four bands expected for the OH ( $\nu = 0-1$ ) spectrum have been made. These bands, at 3133.9 and 3134.9 cm<sup>-1</sup>, have a large frequency shift from free OH, but exhibit little of the intensity increase anticipated if the H bond were intermolecular rather than intramolecular. The narrowness of these bands (4 cm<sup>-1</sup> FWHM) in the cold, isolated molecule is in striking contrast to the broad bands (400 cm<sup>-1</sup> FWHM) often observed for intramolecularly H-bonded OH groups in the room temperature gas phase spectrum.<sup>31</sup>

Unfortunately, the present results do not determine with certainty the OH ( $\nu = 1$ ) tunneling splitting. The interpretation favored by the present results suggests an OH ( $\nu = 1$ ) tunneling splitting of only 12 cm<sup>-1</sup>, with the 3133.9 and 3134.9 cm<sup>-1</sup> transitions terminating in the upper tunneling level of OH ( $\nu = 1$ ). The correctness of this assignment would require the lower tunneling level of OH ( $\nu = 1$ ) to be 5–10 times broader than their observed counterparts terminating in the upper tunneling level. The tantalizing conclusion presented by this tentative assignment is that the OH ( $\nu = 1$ ) tunneling splitting is not particularly large, despite the

anticipated strong coupling of the OH stretch mode with the H-atom tunneling coordinate. If this assignment holds up to future tests, it would suggest that the significant nonlinearity of the intramolecular H bond in tropolone reduces the importance of the OH stretch in promoting H-atom tunneling.

## ACKNOWLEDGMENTS

The authors gratefully acknowledge the Petroleum Research Fund, administered by the American Chemical Society, and the National Science Foundation for their support of this research. R.K.F. thanks Lubrizol for an industrial fellowship which provided support during this research.

- <sup>1</sup>(a) R. L. Redington, Y. Chen, G. J. Scherer, and R. W. Field, *J. Chem. Phys.* **88**, 627 (1988); (b) R. L. Redington, *ibid.* **92**, 6447 (1990); (c) R. L. Redington and C. W. Bock, *J. Phys. Chem.* **95**, 10284 (1991).
- <sup>2</sup>R. L. Redington and T. E. Redington, *J. Mol. Spectrosc.* **78**, 229 (1979).
- <sup>3</sup>Y. Ikegami, *Bull. Chem. Soc. Jpn.* **36**, 1118 (1963).
- <sup>4</sup>Y. Tomioka, M. Ito, and N. Mikami, *J. Phys. Chem.* **87**, 4401 (1983).
- <sup>5</sup>R. Rosetti and L. E. Brus, *J. Chem. Phys.* **73**, 1546 (1980).
- <sup>6</sup>A. C. P. Alves and J. M. Hollas, *Mol. Phys.* **23**, 927 (1972); A. C. P. Alves and J. M. Hollas, *ibid.* **25**, 1305 (1973); A. C. P. Alves, J. M. Hollas, H. Musa, and T. Ridley, *J. Mol. Spectrosc.* **109**, 99 (1985).
- <sup>7</sup>(a) H. Sekiya, Y. Nagashima, and Y. Nishimura, *J. Chem. Phys.* **92**, 5761 (1990); (b) H. Sekiya, Y. Nagashima, T. Tsuji, Y. Nishimura, A. Mori, and H. Takeshita, *J. Phys. Chem.* **95**, 10311 (1991); (c) H. Sekiya, K. Sasaki, Y. Nishimura, Z-H. Li, A. Mori, and H. Takeshita, *Chem. Phys. Lett.* **173**, 285 (1990).
- <sup>8</sup>T. Tsuji, H. Sekiya, Y. Nishimura, R. Mori, A. Mori, and H. Takeshita, *J. Chem. Phys.* **97**, 6032 (1992).
- <sup>9</sup>H. Sekiya, H. Takesue, Y. Nishura, Z-H. Li, A. Mori, and H. Takeshita, *J. Chem. Phys.* **92**, 2790 (1990).
- <sup>10</sup>F. A. Ensminger, J. Plassard, and T. S. Zwier, *J. Phys. Chem.* **97**, 4344 (1993).
- <sup>11</sup>F. A. Ensminger, J. Plassard, T. S. Zwier, and S. Hardinger, *J. Chem. Phys.* **99**, 8341 (1993).
- <sup>12</sup>F. A. Ensminger, J. Plassard, T. S. Zwier, and S. Hardinger, *J. Chem. Phys.* **102**, 5246 (1995).
- <sup>13</sup>J. J. Nash, T. S. Zwier, and K. D. Jordan, *J. Chem. Phys.* **102**, 5260 (1995).
- <sup>14</sup>T. D. Sewell and D. L. Thompson, *Chem. Phys. Lett.* **193**, 347 (1992).
- <sup>15</sup>N. Shida, P. F. Barbara, and J. E. Almöf, *J. Chem. Phys.* **91**, 4061 (1989).
- <sup>16</sup>Th. Walther, H. Bitto, T. K. Minton, and J. R. Huber, *Chem. Phys. Lett.* **231**, 64 (1994).
- <sup>17</sup>(a) Z. S. Huang and R. E. Miller, *J. Chem. Phys.* **91**, 6613 (1989); (b) G. T. Fraser, *Int. Rev. Phys. Chem.* **10**, 189 (1991), and references therein.
- <sup>18</sup>F. Huisken, A. Kulcke, C. Laush, and J. M. Lisy, *J. Chem. Phys.* **95**, 3924 (1991).
- <sup>19</sup>(a) R. N. Pribble and T. S. Zwier, *Science* **265**, 75 (1994); (b) R. N. Pribble and T. S. Zwier, *Faraday Discuss.* **97**, 229 (1994); (c) R. N. Pribble, A. W. Garrett, K. Haber, and T. S. Zwier, *J. Chem. Phys.* **103**, 531 (1995); (d) T. S. Zwier, *Annu. Rev. Phys. Chem.* (1996), Vol. 47, and references therein.
- <sup>20</sup>F. Huisken, M. Kaloudis, and A. Kulcke, *J. Chem. Phys.* **104**, 17 (1996).
- <sup>21</sup>(a) S. Tanabe, T. Ebata, M. Fujii, and N. Mikami, *Chem. Phys. Lett.* **215**, 347 (1993); (b) N. Mikami, *Bull. Chem. Soc. Jpn.* **68**, 683 (1995); (c) T. Watanabe, T. Ebata, S. Tanabe, and N. Mikami, *J. Chem. Phys.* (in press).
- <sup>22</sup>T. Ebata, N. Mizuochi, T. Watanabe, and N. Mikami, *J. Phys. Chem.* (in press).
- <sup>23</sup>S. Djafari, G. Lembach, H.-D. Barth, and B. Brutschy, *Z. Phys. Chemie* (in press).
- <sup>24</sup>G. C. Pimentel and A. L. McClellan, *The Hydrogen Bond* (Freeman, San Francisco, 1960).
- <sup>25</sup>H. Tsubomura, *J. Chem. Phys.* **24**, 927 (1956).
- <sup>26</sup>A. Mitsuzuka, A. Fujii, T. Ebata, and N. Mikami, *J. Chem. Phys.* **105**, 2618 (1996), second following paper.
- <sup>27</sup>M. J. Frisch, G. W. Trucks, H. B. Schlegel, P. M. W. Gill, B. G. Johnson, M. W. Wong, J. B. Foresman, M. A. Robb, M. Head-Gordon, E. S. Replogle, R. Gomperts, J. L. Andres, K. Raghavachari, J. S. Binkley, C. Gonzalez, R. L. Martin, D. J. Fox, D. J. Defrees, J. Baker, J. J. P. Stewart, J. A. Pople, in *GAUSSIAN92, DFT Manual* (Gaussian, Inc., Pittsburgh, PA, 1993).
- <sup>28</sup>(a) A. D. Becke, *J. Chem. Phys.* **98**, 5648 (1993); (b) S. H. Vosko, L. Wilk, and M. Nusir, *Can. J. Phys.* **58**, 1200 (1980); (c) C. Lee, W. Yang, and R. G. Parr, *Phys. Rev. B* **37**, 785 (1988).
- <sup>29</sup>(a) K. Kim, K. D. Jordan, and T. S. Zwier, *J. Am. Chem. Soc.* **116**, 11568 (1994); (b) S. Y. Fredericks, K. D. Jordan, and T. S. Zwier, *J. Phys. Chem.* (in press).
- <sup>30</sup>(a) T. Clark, J. Chandrasekhar, G. W. Spitznagel, and P. v. R. Schleyer, *J. Comput. Chem.* **4**, 294 (1983); (b) W. J. Hehre, R. Ditchfield, and J. A. Pople, *J. Chem. Phys.* **56**, 2257 (1972); (c) M. J. Frisch, J. A. Pople, and J. S. Binkley, *ibid.* **80**, 3265 (1984).
- <sup>31</sup>K. Tanaka, H. Honjyo, T. Tanaka, H. Takaguchi, Y. Ohshima, and Y. Endo, Abstracts of the Meeting on Molecular Structure, Yokohama, Japan 1991 (unpublished), p. 223.
- <sup>32</sup>K. Rutkowski and A. Koll, *J. Mol. Structure* **322**, 195 (1994).
- <sup>33</sup>Z. Smedarchina, W. Siebrand, and M. Z. Zgierski, *J. Chem. Phys.* **104**, 1203 (1996).
- <sup>34</sup>Z. Smedarchina, W. Siebrand, and M. Z. Zgierski (unpublished results).
- <sup>35</sup>M. Quack, *Annu. Rev. Phys. Chem.* **41**, 839 (1990); J. Davidsson, J. H. Gutow, R. N. Zare, H. A. Hollenstein, R. R. Marquardt, and M. Quack, *J. Phys. Chem.* **95**, 1201 (1991).
- <sup>36</sup>A. McIlroy and D. J. Nesbitt, *J. Chem. Phys.* **92**, 2229 (1990).
- <sup>37</sup>J. E. Gambogi, K. K. Lehmann, B. H. Pate, G. Scoles, and S. Yang, *J. Chem. Phys.* **98**, 1748 (1993); B. H. Pate, K. K. Lehmann, and G. Scoles, *ibid.* **95**, 3891 (1991).
- <sup>38</sup>G. A. Bethardy and D. S. Perry, *J. Chem. Phys.* **98**, 6651 (1993); **99**, 9400 (1993); J. Go and D. S. Perry, *ibid.* **103**, 5194 (1995).
- <sup>39</sup>(a) K. B. Hewett, M. Shen, C. L. Brummel, and L. A. Philips, *J. Chem. Phys.* **100**, 4077 (1994); (b) H. Li, C. C. Miller, and L. A. Philips, *ibid.* **100**, 8590 (1994).
- <sup>40</sup>(a) M. Scotoni, S. Oss, L. Lubich, S. Furlani, and D. Bassi, *J. Chem. Phys.* **103**, 897 (1995); (b) M. Scotoni, C. Leonardi, and D. Bassi, *ibid.* **95**, 8655 (1991).
- <sup>41</sup>P. R. Fleming, M. Li, and T. R. Rizzo, *J. Chem. Phys.* **94**, 2425 (1991); X. Luo, P. R. Fleming, T. A. Seckel, and T. R. Rizzo, *ibid.* **93**, 9194 (1990).
- <sup>42</sup>H. Michelsen and P. Klaboe, *J. Mol. Struct.* **4**, 293 (1969); H. Niki, P. D. Maker, C. M. Savage, and M. D. Hurley, *J. Phys. Chem.* **91**, 2174 (1987).